Proceedings of the 8th U.S. National Conference on Earthquake Engineering
April 18-22, 2006, San Francisco, California, USA
Paper No. 1205

DESIGN OF FRP RETROFITTED FLEXURAL MEMBERS AGAINST DEBONDING FAILURES

O. Gunes[1], E. Karaca[2], and B. Gunes[3]

ABSTRACT

Use of fiber reinforced polymer (FRP) composites in seismic retrofitting of structural members has been steadily increasing in recent years. An important design issue with significant performance and safety implications is the debonding of externally bonded FRP reinforcement in flexural members. This paper provides the highlights of an experimental and analytical research aimed at understanding and modeling of debonding failures in FRP strengthened reinforced concrete beams. An evolutionary experimental program investigated debonding failure mechanisms and modes in beams strengthened in shear and/or flexure in various configurations and tested under monotonic and cyclic loading. A newly developed fracture mechanics based model considers the global energy balance of the system and predicts the debonding failure load by characterizing the dominant mechanisms of energy dissipation during debonding. Validation of the model is performed using experimental data obtained from several independent experimental studies.

Introduction

FRP composites are becoming a material of choice in an increasing number of seismic retrofit projects around the world. Depending on the design objectives, these materials can be used to improve the load capacity and/or ductility of structural members. A multi-national effort is underway to develop proper codes and guidelines to set the standards for material selection, design, installation, inspection, maintenance, and repair of FRP applications. Design of structural strengthening applications using externally bonded FRP composites is usually based on conventional design approaches with improvements to account for the presence and characteristics of the FRP material. Nonconventional design issues that are specific to the type of application require special considerations for their proper inclusion in the design process. One such design issue is the debonding problems in externally bonded FRP strengthening applications that has been a concern and a research challenge since the initial development stages of the method (Kaiser, 1989; Meier, 1995; Buyukozturk and Hearing, 1998). Due to the typical premature and brittle nature of debonding failures, inadequately designed strengthening applications may not only become ineffective, but may also reduce the level of safety of the

[1] Asst. Professor, Dept of Civil and Env. Engineering, University of Massachusetts Lowell, Lowell, MA, 01854
[2] Mendenhall Postdoctoral Fellow, U.S. Geological Survey, Denver, CO 80225
[3] Asst. Professor, Dept. of Civil Engineering, Atilim University, Ankara, 06836, Turkey

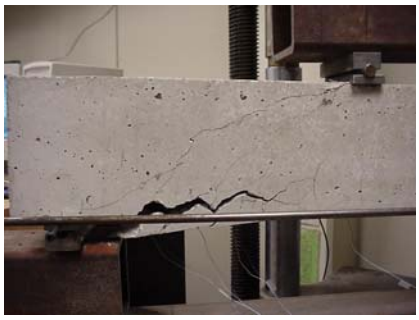

(a) cover debonding

(b) FRP debonding

Figure 1. Debonding failure modes of FRP strengthened beams

member by decreasing its ductility. Design procedures that properly consider debonding problems are needed to ensure the safety and reliability of beams strengthened using FRP composites. This paper presents the highlights of an experimental and analytical study aimed at modeling of FRP debonding failures in retrofitted flexural members and describes the developed design procedure.

Debonding Failure Mechanisms

The term debonding failure is often associated with a significant decrease in member capacity due to initiation and propagation of debonding. Debonding initiation in beams strengthened with FRP composites generally take place in regions of high stress concentration at the concrete-FRP interface. These regions include the ends of the FRP reinforcement, and those around the shear and flexural cracks. The cover debonding mechanism shown in Figure 1(a) is usually associated with high interfacial stresses, low concrete strength, and/or with extensive cracking in the shear span. If the concrete strength and the shear capacity of the beam are sufficiently high, potential debonding failure is most likely to take place through FRP debonding, as shown in Figure 1(b). Depending on the beam parameters and the strengthening configuration, such failures may initiate at the areas of high stress concentration at laminate ends and propagate towards the center of the beam, or may initiate at flexure-shear cracks and propagate towards the ends of the beam. Depending on the material properties, debonding may occur within the FRP laminate, at the concrete-FRP interface, or a few millimeters within the concrete.

Debonding Failure Modeling Research

Characterization and modeling of debonding in structural members strengthened with externally bonded reinforcements has long been a popular area of interdisciplinary research due to critical importance of debonding failures in bonded joints. In the last decade, there has been a concentration of research efforts in this area with respect to FRP strengthened flexural members, and considerable progress has been achieved in understanding the causes and mechanisms of debonding failures through numerous experimental, analytical, and numerical investigations. Modeling research in this area can be classified in general terms by their approach to the problem as strength and fracture approaches. In addition to these, a number of researchers have proposed relatively simple semi-empirical and empirical models that avoid the complexities of stress and fracture analyses and can be relatively easily implemented in design calculations. The

reader is referred to Buyukozturk et al. (2004) for a comprehensive review of debonding failure modeling research. The current guidelines by the ACI Committee 440 enforces a limit on the strain level developed in the FRP reinforcement as a preliminary measure against debonding failures (ACI 440, 2002). This limit is based on expert opinion and depends only on the material properties of the FRP reinforcement. There is a need for a debonding model that can successfully predict debonding failures by considering all relevant member and strengthening parameters.

Experimental Study

The experimental study presented herein is part of a comprehensive experimental program carried out to investigate the monotonic and cyclic load performance of precracked reinforced concrete beams strengthened in flexure and/or shear using FRP composite plates and sheets. The focus of the study is characterization and prevention of debonding failures as affected by the shear strengthening and anchorage conditions. In this paper, a limited number of experimental results that are used in the modeling studies presented in the following sections are provided. Laboratory size reinforced concrete beams were strengthened in shear and/or flexure with and without anchoring of the flexural FRP reinforcement, and were loaded in four-point bending until failure. All beams were precracked prior to strengthening. The geometry and reinforcement details of the control specimen (CM1) is shown in Figure 2(a) and the strengthening configurations of the tested beams are shown in Figure 2(b). All specimens shown in this figure were strengthened with 1270 mm (50 in) long, 38.1 mm (1.5 in) wide, and 1.2 mm (0.047 in) thick FRP plates. For FRP shear strengthening, 40-mm wide straight and L-shaped plates were used. For comparison with external shear strengthening, the shear capacity of a beam was increased through larger internal shear reinforcement (see beam S2PF7M in Figure 2b). Properties of the materials used in the experimental program are given in Table 1.

The load-deflection curves obtained from tests are shown in Figure 3(a) and the corresponding load vs. mid-span FRP strain curves are shown in Figure 3(b). Except for the beam S1PF1M, all beams shown in Figure 2(b) failed through FRP debonding. Beam S1PF1M failed through cover debonding followed by shear failure, although the theoretical shear capacity of the unstrengthened beam was approximately 20 percent higher than the failure load of beam S1PF1M. Comparing the load-deflection curves for beam S1PF1M and S2PF7M, the influence of the shear capacity of a beam on its failure behavior is immediately apparent. Both beams were strengthened in the same configuration and essentially both failed through debonding. However, the failure load of S2PF7M, which had sufficiently high shear capacity, was approximately 15 percent higher than that of beam S1PF1M. The beams strengthened in shear with side bonded

Table 1. Properties of materials used in the experimental program

Material	Compressive strength (MPa)	Yield strength (MPa)	Tensile strength (MPa)	Tensile modulus (MPa)	Ult. tensile strain (%)
Concrete	41.4	-	-	-	-
#3 and #5 rebars	-	440	-	200,000	-
D4 deformed bars	-	620	-	200,000	-
CFRP plate	-	-	2800.0	165,000	1.69
Epoxy adhesive	-	-	24.8	4,482	1.00

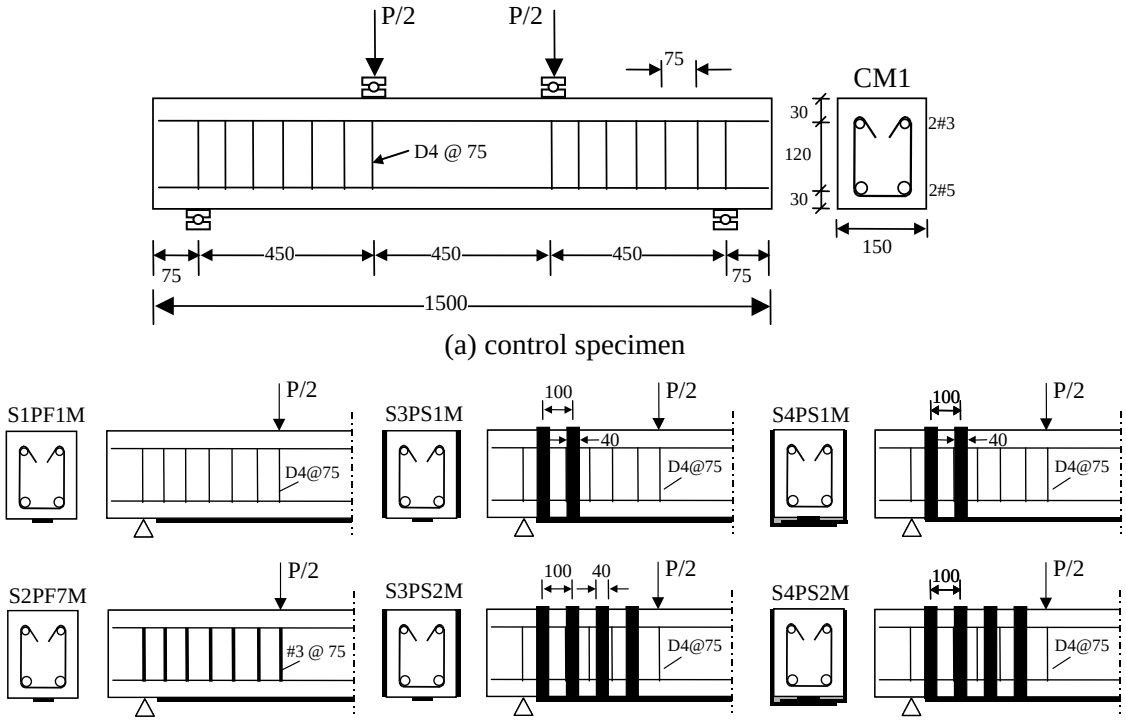

(a) control specimen

(b) beams strengthened in shear and/or flexure in various configurations

Figure 2. FRP retrofitted test beam specimens

plates along the half and full shear span, S3PS1M and S3PS2M, respectively, displayed essentially the same performance as S2PF7M. This suggests that the shear capacity of a strengthened beam is especially critical in the plate-end region, where the flexure-shear cracks initiated at plate ends propagate higher into the beam. The influence of shear strengthening combined with anchorage of the flexural reinforcement, which was achieved by L-shaped plates, was significant as shown in Figure 3(b). Unlike the case for side bonded plates, increasing L-shaped plate bonding from half shear span to full shear span resulted in a large performance increase due to increased bond area and fracture surface.

For the particular FRP reinforcement used, the limiting effective strain is calculated in accordance with the ACI 440 (2002) guide as $\varepsilon_{fe} = 0.0076$, which is shown with a dashed line as the ACI limit in Figure 3(b). Comparison of this strain limit with the experimental results indicate that this calculated strain limit is nonconservative in most cases. The practical strain limit recommended by the manufacturer, $\varepsilon_{fe} = 0.006$ provides a better estimation of the FRP strain at debonding since this limit is based on targeted experimental studies using the particular reinforcement. However, Figure 3(b) shows that this limit cannot be considered as generally applicable since it is nonconservative for case of beam S1PF1M which failed through cover debonding at an FRP strain level of 0.004. It should also be noted that the practical strain limit is over-conservative for beams with bond anchorage (S4PS1M and S4PS2M) which has economic significance.

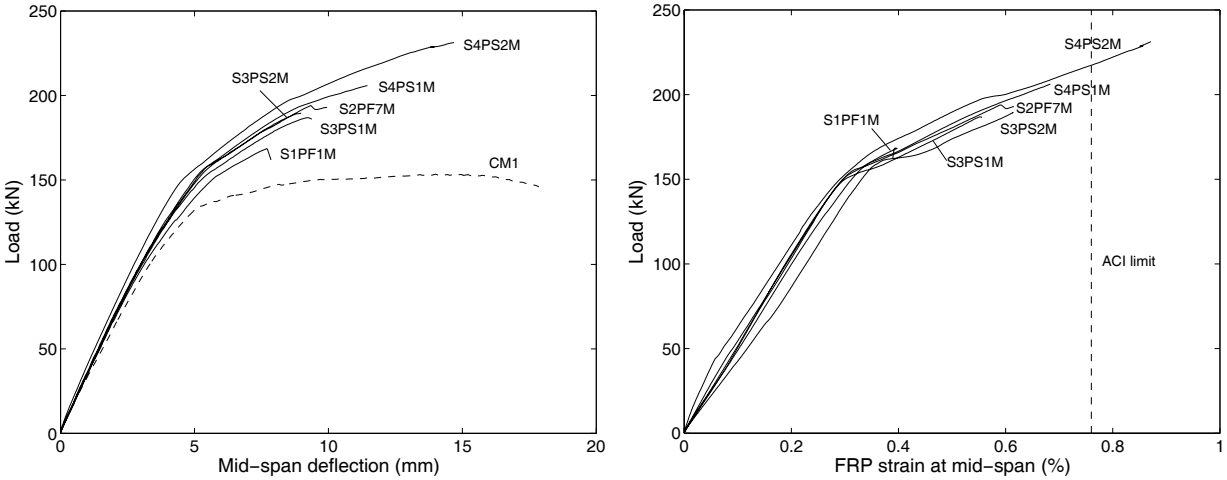

(a) load-deflection curves (b) load vs. mid-span FRP strain curves

Figure 3. Load vs. mid-span deflection and FRP strain curves

Retrofitted Beam Performance under Monotonic and Cyclic Loading

The performance of strengthened members under cyclic loading is of great importance for seismic retrofit applications. Figure 4 shows a comparison of performance under monotonic and cyclic loading for two retrofit configurations. In the first configuration shown in Figure 4(a), the beam is strengthened using flexural and side bonded FRP reinforcement without bond anchorage (see specimen S3PS2M in Figure 2b). In the second configuration shown in Figure 4(b), the shear strengthening is performed using L-shaped composite FRP plates to provide bond anchorage for the flexural FRP reinforcement (see specimen S4PS2M in Figure 2b). The cyclic tests are performed as displacement controlled with 0.5 mm increments up to 10 mm total mid-span deflection, and 1 mm increments thereafter. No reverse loading is applied since the simply supported test configuration represents the portion of a real-life beam between the inflection points, which typically is not subjected to reverse loading around the center span under combined design loading. Comparison of load deflection curves in each case shows that providing bond anchorage for the flexural reinforcement not only improves the load capacity, but also increases the cyclic load performance of the beam. Without bond anchorage, bond degradation is more likely to occur under low amplitude cyclic loading, which reduces the performance of the retrofitted member under high amplitude cyclic loading, such as during earthquakes.

A Fracture Model for FRP Debonding

Debonding and associated fracture processes result in global energy transformations in FRP strengthened members. In the early stages of loading, these fracture processes may be gradual and stable, whereas upon reaching a critical energy state, a sudden brittle failure may takes place. The mechanisms of energy dissipation in FRP strengthened RC beams under loading include cracking and crushing of concrete, reinforcement yielding and pullout, and FRP

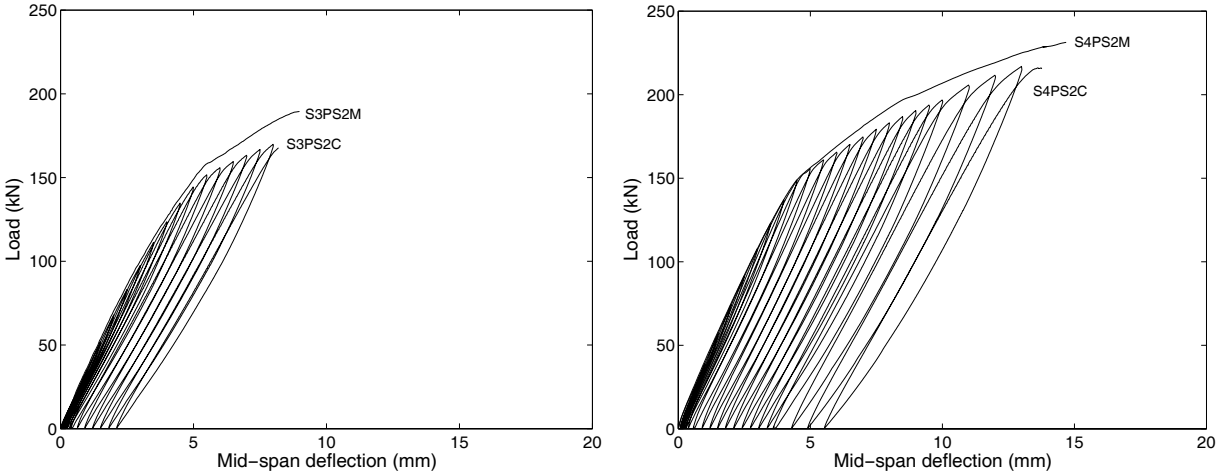

(a) flexure+shear strengthening without anchorage (b) flexure and shear strengthening with anchorage

Figure 4. Comparison of retrofitted beam performance under monotonic and cyclic loading

debonding. Debonding failure in beams may take place before or after steel reinforcement yielding depending on the reinforced concrete beam geometry and FRP strengthening configuration. The potential energy difference in strengthened beams upon debonding failure is depicted in Figure 5 for the cases of before and after reinforcement yielding. The difference between Figure 5 (a) and (b) in terms of energy dissipation is that the latter involves and added plastic energy dissipation due to reinforcement yielding. Assuming that the bulk energy dissipation ($\int \Upsilon d\Omega$) due to damage away from the concrete-FRP interface is insignificant, the total energy dissipation, $\Delta\mathcal{D}$, given by the negative change in potential energy during debonding failure can be approximated as:

$$\Delta\mathcal{D} \approx \int \sigma \cdot d\varepsilon^p d\Omega + \int G_f A_f \geq 0 \; ; \quad \varepsilon^p = \varepsilon_s - \varepsilon_y \geq 0 \tag{1}$$

where $\int \sigma \cdot d\varepsilon^p d\Omega$ is the plastic energy dissipation due to steel yielding when $\varepsilon_s > \varepsilon_y$ and is equal to zero otherwise. The term $\int G_f dA_f$ represents dissipation due to debonding process evaluated over the crack surface defined by the energy per unit area necessary for the crack formation called the interface fracture energy G_f, and the interfacial bond area A_f.

Figure 6(b) shows that the beam deflection and thus the curvature essentially stays constant upon debonding, which can be used to derive the plastic energy dissipation during debonding through yielding of the steel reinforcement as:

$$W_s^p = \int \sigma \cdot d\varepsilon^p d\Omega = \sigma_s \Delta\varepsilon_s A_s l_s = f_y \varepsilon_c (1 - \frac{c'}{c}) A_s l_c \tag{2}$$

where ε_c is the maximum concrete strain, and *c* and *c'* are the neutral axis depth before and after debonding, respectively, A_s is the total cross-sectional area of the steel reinforcement and l_c is the length of the constant moment region.

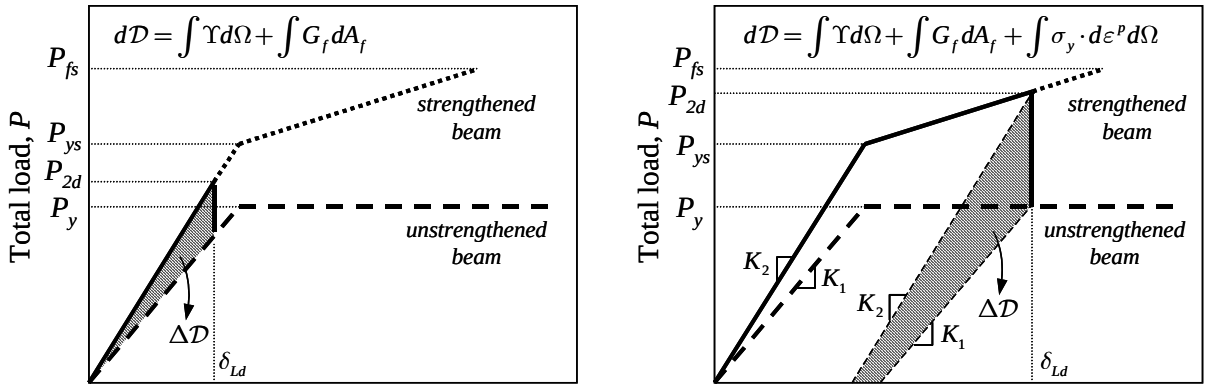

(a) before steel reinforcement yielding (b) after steel reinforcement yielding

Figure 5. Energy dissipation during debonding failure

The energy dissipated at the FRP concrete interface region during debonding goes to creating new surfaces along the bond area. Depending on the fracture properties of the materials that form the strengthened system, debonding fracture may take place within or at the interfaces of the materials, taking the path that requires the least amount of energy. Assuming pure mode II fracture along FRP-concrete and FRP-FRP interfaces, the debonding energy dissipation term in Eq.(1) can be written as:

$$\int G_f dA_f \approx \int G_{FII} dA_{fb} + \int \Gamma_{FII} dA_{fa} \tag{3}$$

where G_{FII} and Γ_{FII} are the mode II fracture energies of concrete-FRP and FRP-FRP bond interfaces which are approximated as 1400 joules/m^2 and 2800 joules/m^2, respectively, $A_{fb} = l_f b_f$ is the bond area at the FRP-concrete interface and $A_{fa} = l_a b_a$ is the bond area between the flexural FRP reinforcement and the transverse FRP shear reinforcement that is providing bond anchorage.

Using Eqs. (1)-(3) a global debonding criterion can be developed based on the assumption that debonding takes place along the entire bond surface along the FRP reinforcement with concrete and if present with the transverse anchorage reinforcement:

$$\Delta\mathcal{D} = \frac{P_{2d}^2}{2K_2} - \frac{P_y^2}{2K_1} = (G_{FII} l_f b_f + \Gamma_{FII} l_a b_a) + W_s^p \geq 0 \quad (P_{2d} > P_y) \tag{4}$$

where $P_{2d} = P(\delta_L = \delta_{Ld})$ and $P_{1d} = P(\delta_L = \delta_{Ld}) = P_y$ are the load values for before and after debonding that takes place at deflection δ_{Ld} under the load application points. The stiffness values for the strengthened and unstrengthened beams, K_2 and K_1 respectively, are given by:

$$K_2 = 2EI_2 \Big/ \left[\frac{l_s^2 L}{2} - \frac{2l_s^3}{3}\right], \quad K_1 = 2EI_1 \Big/ \left[\frac{l_s^2 L}{2} - \frac{2l_s^3}{3}\right] \tag{5}$$

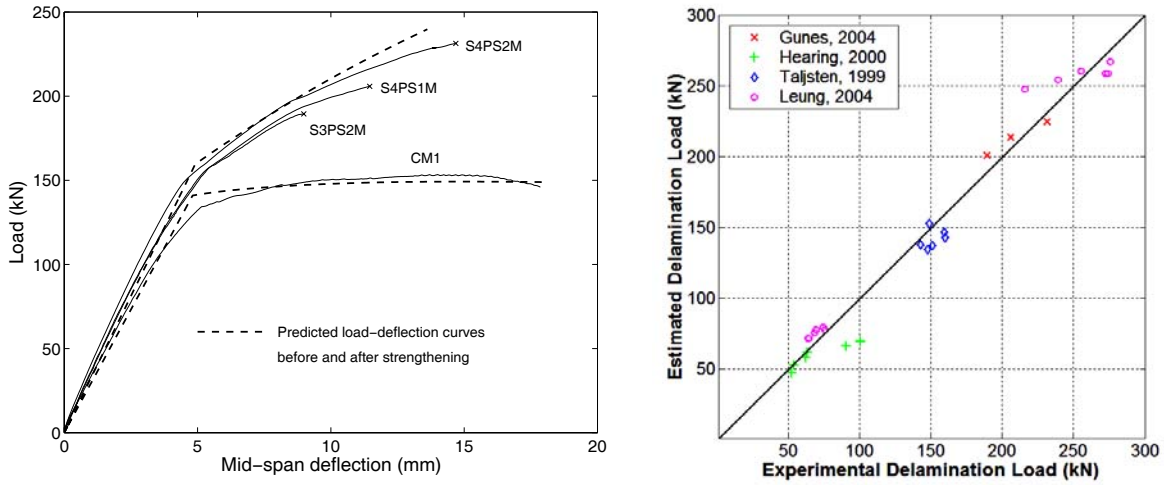

(a) experimental results (b) validation with experimental results

Figure 6. Comparison of debonding model predictions with multiple sets of experimental results

where I_1 and I_2 are the cracked moment of inertias of the transformed beam sections, and l_s is the shear span.

Eq. (4) indicates that for increasing beam curvature/deflection under loading, the portion of the energy stored in the strengthened beam in excess of that stored in the unstrengthened beam reaches a critical value that causes debonding failure and its dissipation through reinforcement yielding and debonding fracture. This criterion can be used to determine the debonding load level based on beam and strengthening parameters.

Validation of the developed model was performed using experimental results obtained from this and various other independent experimental studies to compare the model prediction with the experimental results. The reader is referred to Gunes (2004) for details of the correction and calibration of the experimental results obtained from the presented flexural tests. Figure 7(a) shows the experimental results obtained from representative beam tests within the presented research (excluding the cover debonding failure case) together with the nonlinear load-deflection curves for the control and strengthened beams. A comparison of the model predictions with the experimental results obtained from various independent experimental studies (Taljsten, 1999; Hearing, 2000; Leung, 2004) is shown in Figure 7(b). As can be seen from the figure, the developed fracture model yields a satisfactory prediction of the FRP debonding failure loads. The overall success of the model in predicting FRP debonding failure loads for various sizes of beams and strengthening configurations shows the potential of fracture mechanics modeling approach for design against debonding failures.

Design of Flexural Members against FRP Debonding Failures

The developed FRP debonding failure model can easily integrated into design of FRP strengthened beams to achieve safety against FRP debonding failures. The design approach is described in the following steps starting from the design of FRP strengthened beams for flexure and shear effects:

1. Perform the strengthened beam design using conventional ultimate strength analysis for design flexural loads (ACI 440, 2002). The outcome of this step is the cross-sectional area of the bonded FRP reinforcement $A_f = b_f t_f$ needed for strengthening.

2. Perform design for shear strengthening of the beam using side bonded or wrapped FRP composites if the design shear load exceeds the beam shear capacity.

3. In order to ensure ductile behavior and failure of the beam, equate the debonding failure design load to the flexural capacity of the beam calculated in step 1, and calculate the total bond fracture resistance needed to resist the debonding failure load using Eq. (4):

$$\mathcal{D}_d = (G_{FII} l_f b_f + \Gamma_{FII} l_a b_a) = \frac{P_{2d}^2}{2K_2} - \frac{P_y^2}{2K_1} - W_s^p \geq 0 \tag{6}$$

4. Once the required total debonding energy is determined, one has to make sure that the total fracture energy of the FRP-concrete bond and possible anchorage is sufficient to meet this energy demand. Since the required FRP reinforcement area A_f is known from step 1, the first try would be to check if the bond area of the FRP (plate) reinforcement designed in step 1 is sufficient (or to arrange the width and thickness of the FRP (sheet) reinforcement to provide sufficient bond area) without any anchorage:

$$b_f = \frac{\mathcal{D}_d}{G_{FII} l_f} \leq b, \quad t_f = \frac{A_f}{b_f} \tag{7}$$

   Special attention must be paid not to design the FRP reinforcement too thin to avoid FRP rupture due to stress concentrations at crack locations. If the bond area without any anchorage is not enough to meet the energy demand, then anchorage requirement needs to be calculated to provide additional fracture energy:

$$l_a b_a = \frac{\mathcal{D}_d - G_{FII} l_f b_f}{\Gamma_{FII}} \tag{8}$$

   so that the integrity of the bond is ensured under the design load. The calculated anchorage reinforcement should be placed close to the FRP reinforcement end regions.

It should be noted that the developed FRP debonding model does not address cover debonding failures since this failure type appears to be mainly influenced by the shear behavior and capacity of the beam. Until an accurate model is developed to address cover debonding failures, specification of a minimum bond anchorage in the FRP reinforcement end regions with a length approximately equal to the beam height is recommended as a safety assurance.

Conclusions

A global fracture model was developed through experimental research and analytical modeling studies to predict FRP debonding failures in strengthened flexural members. The model includes the member geometry, strengthening configuration, and additional bond anchorage effects considering energy balance in the system and energy dissipation through steel

reinforcement yielding and FRP debonding. Implementation of the model to several sets of independently reported experimental data shows that the model can satisfactorily predict the FRP debonding failure loads for various sizes of beams strengthened in various configurations, with or without bond anchorage. The model can be further improved through better characterization of its components such as bulk energy dissipation in the concrete beam during debonding, and mixed mode fracture energy values at the FRP-concrete and FRP-FRP interfaces.

Experimental results obtained from monotonic and cyclic load testing of retrofitted beams revealed that providing bond anchorage for the flexural FRP reinforcement plays a significant role in cyclic load performance. Reduction in the load capacity under cyclic loading was observed to be considerably higher for beams without bond anchorage compared to those with bond anchorage by means of L-shaped FRP plates. As a result of several cyclic load tests for various strengthening configurations, it is recommended that a minimum bond anchorage is provided at the end regions of the FRP flexural reinforcement along a distance equal to the beam depth to ensure improved cyclic load performance.

The developed model can easily be integrated into the design of FRP retrofitted flexural members to ensure safety against FRP debonding failures. With further improvements to included cover debonding failure and further validation, the model may be used as a code provision for preventing debonding failures.

References

ACI 440 (2002), *Guide for the Design and Construction of Externally Bonded FRP Systems for Strengthening Concrete Structures*, ACI 440.2R-02, American Concrete Institute, Detroit.

Buyukozturk, O., and Hearing, B. (1998), "Failure Behavior of Precracked Concrete Beams Retrofitted with FRP," *Journal of Composites for Construction*, Vol. 2, No. 3, pp. 138-144.

Buyukozturk, O., Gunes, O, and Karaca, E. (2004), “Progress Review on Understanding Debonding Problems in Reinforced Concrete and Steel Members Strengthened Using FRP Composites,” *Construction and Building Materials*, Vol 18, pp. 9-19.

Gunes, O. (2004), A Fracture Based Approach to Understanding Debonding in FRP Bonded Structural Members, Ph.D. Thesis, Massachusetts Institute of Technology, Cambridge, MA.

Hearing, B. (2000), *Delamination in Reinforced Concrete Retrofitted with Fiber Reinforced Plastics*, Ph.D. Thesis, Massachusetts Institute of Technology, Cambridge, MA.

Kaiser, H. P. (1989), “Strengthening of Reinforced Concrete with Epoxy-Bonded Carbon Fibre Plastics,” *Doctoral Thesis*, Diss. ETH Nr. 8918, ETH Zurich, Switzerland, (in German).

Leung, C.K.Y. (2001), “Delamination Failure in Concrete Beams Retrofitted With a Bonded Plate,“ *Journal of Materials in Civil Engineering*, Vol. 13, No. 2, pp. 106-113.

Leung C. K. Y. (2004), Unpublished experimental data through personal communication, Hong Kong University of Science and Technology, Kowloon, Hong Kong.

Meier, U. (1995), “Strengthening of Structures using Carbon Fibre/Epoxy Composites,” *Construction and Building Materials*, Vol. 9, No. 6, pp. 341-351.

Taljsten, B. (1999), “Concrete Beams Strengthened for Bending Using CFRP-Sheets,” *Structural Faults + Repair-99*, Forde, M.C. (Ed.), London, UK.